# Raman scattering on ZnO nanocrystals

J. Marquina
*Centro de Estudios Avanzados en Óptica, Facultad de Ciencias,*
*Universidad de los Andes, Mérida 5101, Venezuela.*

Ch. Power and J. González
*Centro de Estudios de Semiconductores, Facultad de Ciencias,*
*Universidad de los Andes, Mérida 5101, Venezuela.*

We present here a novel and simple physical method for obtaining ZnO nanocrystals using the pressure cycle method and the membrane diamond anvil cell (MDAC) up to 13 GPa at 500 K. The recovered nanocrystals in the wurtzite phase (w–ZnO) were characterized by high resolution Raman scattering and XRD studies. Single crystal of the w–ZnO was used in this work. The high–pressure cell was a membrane DAC specifically designed for high–temperature studies. The Raman spectra of high quality ZnO single crystal and nanocrystals were compared, and we observed both the softening and the asymmetric broadening of Raman peaks, which are in good agreement with the effect of relaxation of the q–vector selection rule due to quantum size confinement effect. The experimental results confirms the existence of ZnO nanocrystals in the wurtzite phase with a diameter of the order of 17 nm.

*Keywords:* Nanocrystals; II–VI semiconductors; ZnO.

Nosotros presentamos aquí un método original y simple para obtener nanocristales de ZnO utilizando el método de ciclo de presión y la celda con yunques de diamante de memebrana (MDAC) hasta los 13 GPa a 500 K. Los nanocristales recuperados en la fase Wurtzita (w–ZnO) fueron caracterizados mediante dispersión Raman de alta resolución y estudios de difracción de rayos X (XRD). En este trabajo fueron usados monocristales de w–ZnO. La celda de alta presión fué una DAC de membrana diseñada específicamente para estudios a altas temperaturas. Cuando se compara el espectro Raman de monocristales de ZnO de alta calidad con el de los nanocristales observamos que tanto el ablandamiento como el ensanchamiento asimétrico de los picos Raman estan en correspondencia con la relajación de las reglas de selección del vector–q debido a los efectos cuánticos del confinamiento espacial. Los resultados experimentales confirman la existencia de nanocristales de ZnO en la fase Wurtzita con un diámetro del orden de 17 nm.

*Descriptores:* Nanocristales; semiconductores II-VI; ZnO.

PACS: 61.46.Hk; 78.30.-j; 78.55.Et

## 1. Introduction

With a direct band gap of 3.4 eV at ambient conditions, wurtzitic ZnO (w-ZnO), like GaN or 6H-SiC, is intensively studied in view of potential applicability in the field of opto-electronics (eg, laser or light–emitting diodes) [1]. Furthermore, in comparison with its previous competitors, w–ZnO combines several unique electrical, acoustic, and chemical properties, which make it one of the most technologically relevant binary compounds [2].

The interest in semiconductors, which are spatially confined to a few tens of nanometers, has increased in recent years. Three dimensionally confined electron-hole systems, known as quantum dots (QD), have unusual optical properties that may lead to greatly improved opto–electronic devices [3]. Phonon confinement occurs when d (diameter) is small enough to consider the phonon described by a wave packed instead of a plane wave [4–6]. Several high-pressure structural investigations of ZnO have been done in the last two decades and all agree that the w–ZnO to NaCl–ZnO transition is reversible at ambient temperature (with a transition pressure of 9 GPa upon increasing pressure and 2 GPa upon decreasing pressure). The transition is a first–order reconstrutive transition with a 20 % decrease in unit cell volume and a change in coordination number from 4 to 6.

The ZnO is a material with a Wurtzite structure, space group P6$_3$mc with two chemical formulas for unitary cell. The optical phonons at point $\Gamma$ of the first Brillouin zone belongs to the following irreducible representations

$$\Gamma(\text{opt}) = 1A_1 + 2B_1 + 1E_1 + 2E_2.$$

Both $A_1$ and $E_1$ modes are polar and split into transverse TO and longitudinal optical LO phonons with different frequencies due to the macroscopic electric fields associated with the LO phonons. The short–range interatomic forces cause anisotropy, and $A_1$ and $E_1$ modes have different frecuencies. Because the electrostatic forces dominate the anisotropy in the short–range forces, the TO–LO splitting is larger than the $A_1$ $E_1$ splitting. For the lattice vibrations with $A_1$ and $E_1$ symmetry, the atoms move parallel and perpendicular to the c–axis, respectively. Both $A_1$ and $E_1$ modes are Raman and IR active. The two non-polar IR inactive $E_2$ ($E_{2\text{low}}$, $E_{2\text{high}}$) are Raman active. The $B_1$ modes are IR and Raman inactive (silent modes).

## 2. Experiment

In the up-stroke cycle (black points) at 500 K (view Fig. 1), the pressure of the phase trasition Wurtzite–Rocksalt is ap-

proximataly 8 GPa. In the down–stroke cycle, the transition NaCl–Wurtzite (white points) occurs at 3 GPa [4].

The nanocrystals were formed loading the membrane diamond anvil cell (MDAC) with a single crystal of ZnO. The DAC was surrounded by a heater and a thermocouple was glued on one end of the diamond anvil to determine the average temperature on the sample with an accuracy of 20 K. BN powder was used as a pressure transmitting medium because it is chemically inert in this temperature range. The pressure was measured with the luminescence of the ruby and the accuracy was better than 1 GPa at the maximum pressure reached. Unpolarized micro–Raman scattering measurements were performed in a XY 800 Dylor System equipped with $N_2$ cooled charge coupled device (CCD) detector, in the backscattering geometry. The 514.5 nm line of an Argon laser was used at a power of 5 mW incident on the sample and proved to be low enough to avoid a spurious effect caused by the laser induced heating of the sample. Once loaded, the cell was heated to 500 K and the pressure was increased up to 13 GPa (NaCl–phase). At this point of the thermodynamic cycle, the pressure on the sample remained constant during 20 minutes, and after that, the pressure was decrased to the atmospheric value, and finally we decreased the temperature to 300 K.

To evaluate the grain size, ZnO was measured with D5000 SIEMENS powder diffractometer, using $CuK\alpha_1$ radiation; the instrumental broadening was 0.08°

## 3. Results and discussion

### 3.1. X RD Studies

Figure 2 shows the X-ray diffraction patterns of ZnO. Diffraction lines of nanocrystals show a significant increase of the linewidths compared with those of single crystals. To estimate $d$, one can use Scherrrer's equation [11] expressed by

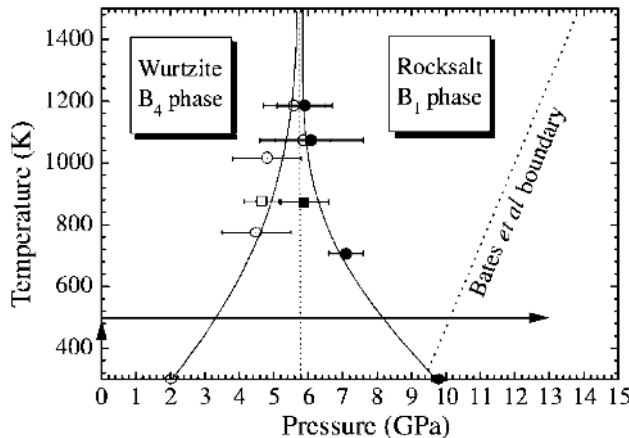$$d = \frac{0.9\,\lambda}{B\cos\Theta_B}, \qquad (1)$$



FIGURE 1. Phase diagram of the ZnO [4]. The lines are to guide the eyes and show Up-stroke cycle and Down-stroke cycle at 500 K.

TABLE I. The values of $d$ for the first six diffraction lines.

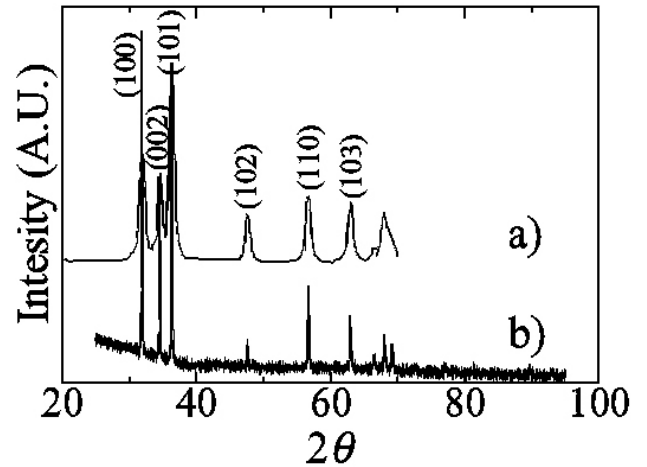| hkl | $2\Theta_B$ | $W$ | $W_0$ | $d$ [nm] |
|-----|-----|-----|-----|-----|
| 100 | 31.9 | 1.0 | 0.1 | 14 |
| 002 | 34.5 | 0.8 | 0.2 | 19 |
| 101 | 36.3 | 0.9 | 0.2 | 17 |
| 102 | 47.6 | 0.9 | 0.2 | 17 |
| 110 | 56.7 | 0.9 | 0.1 | 18 |
| 103 | 63.0 | 0.9 | 0.1 | 18 |



FIGURE 2. X–ray diffraction pattern of ZnO a) nanocrystals and b) single crystals.

where $B$ is an effective linewidth, calculated according to the relation $B^2 = W^2 - W_0^2$, where $W$ and $W_0$ are the FWHM of each diffraction line for the sample after compression (nanocrystals) and before compression (single crystals), respectively, $\lambda$ is the X-ray wavelength and $\Theta_B$ is the Bragg angle. The values of $d$ depend on which diffraction line is chosen. We have calculated $d$ for six diffraction lines (view Table I). The average value is $d = 17$ nm.

### 3.2. Raman Scattering

As compared to the Raman spectrum of high quality ZnO single crystal (see Fig. 3), the phonon confinement of ZnO nanocrystals should affect the phonon energy (red shift) and asymmetry on the low frecuency side. Raman scattering measurements confirm the existence of ZnO nanocrystals in the wurtzite phase. In Fig. (4) we show the raman spectra of the $E_{2low}$ phonon where the confinement effect is cleary observed. To estimate the diameter $d$ of the nanocrystals, we can use the model of confinement proposed by Richter *et al.* [3] and Campbell Fauchet [7], in which the fist order Raman spectrum is given by

$$I(\omega, d) = A' \int\int\int \frac{|C(q)|^2 d\mathbf{q}}{[\omega - \omega(\mathbf{q})]^2 + (\Gamma_0/2)^2}. \qquad (2)$$

In order to simplify the calculations, we use a spherical Brillouin zone, so that,

$$I(\omega, d) = A \int_0^{2\pi/a} \frac{q^2 |C(q)|^2 dq}{[\omega - \omega(q)]^2 + (\Gamma_0/2)^2}. \quad (3)$$

where $A$ is the intensity prefactor, $\omega(q)$ is the phonon dispersion curve, $\Gamma_0$ is the natural full width at half maximum (FWHM), including the instrumental resolution, and $C(q)$ is the Fourier component of the phonon confinement function which is taken as Gaussian, that is,

$$|C(q)|^2 = e^{\left(-\frac{qd}{4\pi}\right)^2}. \quad (4)$$

The phonon dispersion for ZnO has been measured [8], we fit $E_{2low}$ and $E_{2high}$ modes along the $\Gamma$–$A$ direction, with the following expression

$$\omega(q) = \frac{\omega(0)}{\sqrt{2}} \sqrt{1 + \sqrt{1 - \gamma^2 \sin^2(qc/2)}}, \quad (5)$$

where $c$ is the lattice parameter ($c$ being the ZnO lattice parameter $c = 5.21$ Å), $\omega(0)$ is zone–center phonon frequency, and $\gamma$ is a parameter related to the constants of forces. The values $\gamma$ obtained for the $E_{2low}$ and $E_{2high}$ modes were of 0.956 and 0.415, respectively.

Fitting Eq. 3 to the experimental $E_{2low}$ and $E_{2high}$ peaks (see Fig. 5) results in $d = 17.2$ nm and $d = 17.3$ nm, respectively. Table II shows light differences between experimental FWHM ($\Gamma_0$ (exp.)) and FWHM calculated ($\Gamma_0$ (calc.)). Kobayashi et al. [10] have attributed this additional broadening in the experimental width to extrinsic factors. Nevertheless, we observe that this difference is within the experimental error ($\pm 0.6$ cm$^{-1}$).
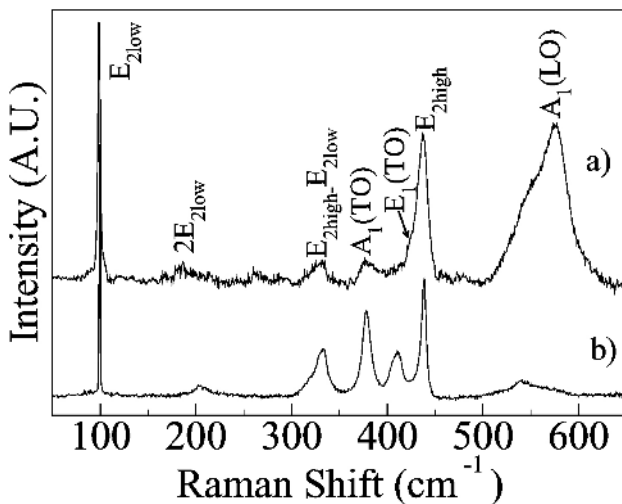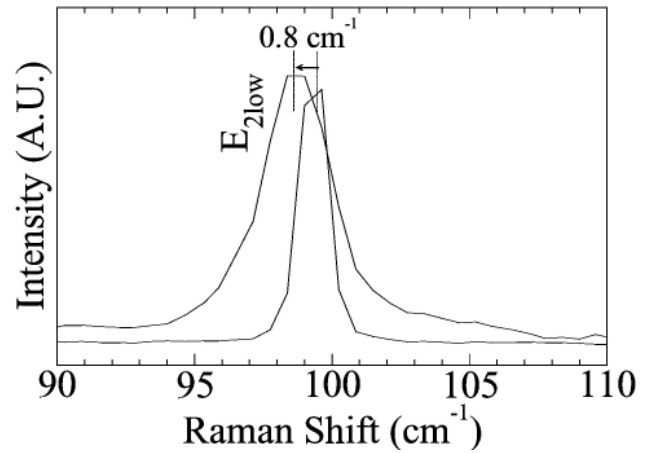


FIGURE 4. Confinement effect on the $E_{2low}$ phonon. The arrow indicates the shift towards a wavenumber lower in the nanocrystaline sample.
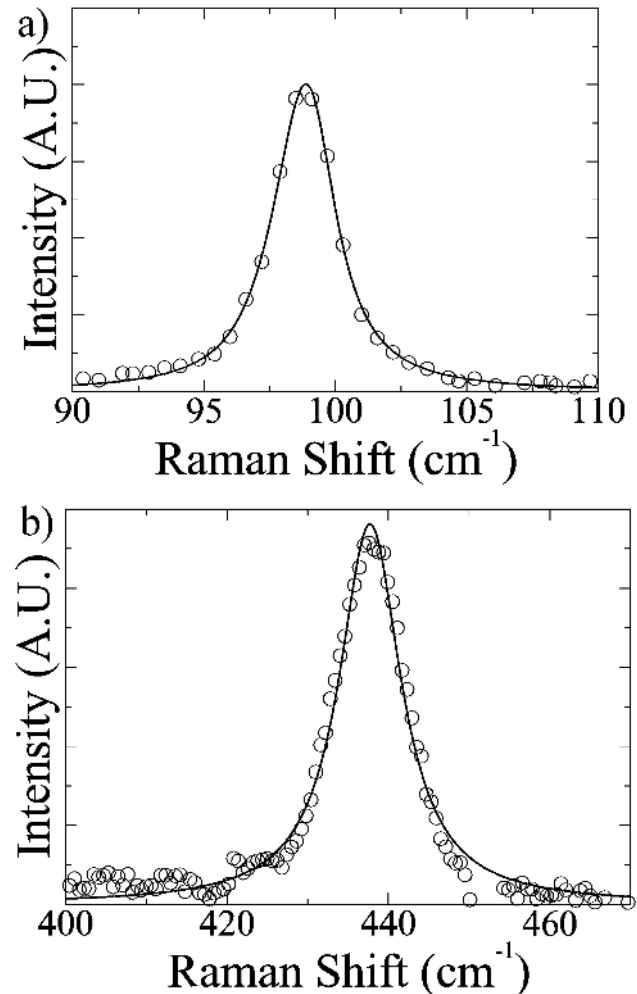


FIGURE 5. Calculated and experimental Raman spectra of ZnO nanocrystals for the a) $E_{2low}$ and b) $E_{2high}$ modes. Open circle: experimental spectra, full curve: calculated spectra using Eq. (3).



FIGURE 3. Raman spectrum of ZnO a) nanocrystals and b) single crystals, excited using a 514.5 nm line of an argon ion laser.

TABLE II. Phonon frequencies, natural linewidths and particle sizes of $E_{2low}$ and $E_{2high}$ modes.

| Optical Phonon | $\omega_0 \left(cm^{-1}\right)$ Reported[a] | $\omega_0 \left(cm^{-1}\right)$ Present work | $\Gamma_0$ (exp.) $[cm^{-1}]$ | $\Gamma_0$ (calc.) $[cm^{-1}]$ | Particle Size [nm] |
|---|---|---|---|---|---|
| $E_{2low}$ | 101 | 99.4 | 2.8 | 2.4 | 17.2 |
| $E_{2high}$ | 444 | 438.2 | 9.3 | 9.2 | 17.3 |

[a]Ref. [9]

## 4. Conclusions

We present here a novel and simple physical method for obtaining ZnO nanocrystals using the pressure cycle method and the membrane diamond anvil cell (DAC) up to 13 GPa at 500 K. The recovered nanocrystals in the wurtzite phase (w–ZnO) were characterized by high resolution Raman scattering and X-ray diffraction. An asymmetric broadening and shifts toward lower frequency in both phonons ($E_{2low}$ and $E_{2high}$ modes)were observed in the Raman spectrum. Similarly, in the X–ray diffraction pattern, a broadening and shift of peaks toward a higher angle were observed. The measured spectra are in good agreement with the ones calculated using a confinement model, and the particle size of 17 nm estimated from the line shape analysis is in good agreement with that found from X–ray analysis.

## Acknowledgements

1. H. Kawazoe *et al.*, *Nature* **389** (1997) 939.

2. D.C. Look, Matter, *Sci. Eng.* **B80** (2001) 383.

3. H. Richter, Z.P. Wang, and L. Ley, *sol. stat. commun.* **39** (1981) 625.

4. F. Decremps, J Zhang, and R. Liebermann, *Europhys. Lett.* **51** (2000) 268.

5. E. Roca, C. Trallero-Giner, and M. Cardona, *Phys. Rev. B* **49** (1994) 13704.

6. M P. Chamberlain, C. Trallero-Giner, and M. Cardona, *Phys. Rev. B* **51** (1995) 1680.

7. I.H. Campbell and P.M. Fauchet, *sol. stat. commun.* **58** (1986) 739.

8. W. Wegener and S. Hautecler, *Phys. Lett. A* **31** (1970) 2.

9. C.A. Arguello, D.L. Rousseau, and S.P. Porto, *Phys. Rev.* **181** (1969) 1351.

10. M. Kobayashi, H. Iwata, H. Hanzawa, T. Yoshiue, and S. Endo, *phys. stat. sol. (b)* **198** (1996) 515.

11. B.D. Cullity, *Elements of X-Ray Diffraction*, Addison–Wesley, 1956.